Resonance ($\Delta\Delta$) degrees of freedom in the deuteron and their influence on the electromagnetic form factors*

M. Gari
Max-Planck-Institut für Chemie, Mainz, Kernphysikalische Abteilung, Germany and Institut für Theoretische Physik, Ruhr-Universität Bochum, Germany

H. Hyuga and B. Sommer†
Institut für Theoretische Physik, Ruhr-Universität Bochum, Germany
(Received 8 July 1976)

The influence of resonance (Δ) contributions on the electromagnetic form factors of the deuteron is calculated. The deuteron wave functions including resonance ($\Delta\Delta$) contributions are determined by a solution of six coupled equations. The effect of various baryon-baryon potentials is discussed. The numerically discussed deuteron electromagnetic form factors include also the meson-exchange contributions arising from π, ρ, and ω pair currents as well as from the $\rho\pi\gamma$ current.

[NUCLEAR REACTIONS ^{2}H(e, e'), resonance admixtures, $d\sigma/d\Omega$ calculated with meson-exchange corrections.]

I. INTRODUCTION

Since the recently performed high energy electron-deuteron scattering experiments[1] renewed interest has arised in the understanding of the deuteron electromagnetic form factors[2-5] by including meson-exchange currents. In view of these results the determination of the neutron form factors also has been pushed further.[6] All these calculations have been performed in a conventional nonrelativistic description of the deuteron. As the exact short-range behavior of these functions is not known a discussion of several very different potentials such as Hamada-Johnston, Reid soft core, or supersoft core has been chosen.[4,5] It turned out that in contrast to the impulse approximation results the total form factors including meson-exchange currents, as π, ρ, ω, and $\rho\pi\gamma$ exchange, are much less sensitive to the choice of the NN potential because of the dominance of the exchange currents at high momentum transfer. Although this kind of calculation of the deuteron form factors did not take care of relativistic corrections[7,8] or inner degrees of freedoms of the deuteron, as for example, the excitation of baryon resonances,[9-11] the theoretical results were found in good agreement with the experimental data.

In the present paper we investigate the influence of baryonic degrees of freedom in the deuteron on the elastic form factors by the inclusion of $\Delta\Delta$ components. The main question to be answered is how strong do the $\Delta\Delta$ components in the deuteron alter the electron-deuteron form factors? The answer to this question seems to be very important because of at least two reasons. Firstly, as the neutron form factors are extracted from the deuteron one hopes that the $\Delta\Delta$ components turn out to be unimportant because otherwise the determination of the neutron form factors will become nearly impossible. On the other hand, in order to study the importance of the $\Delta\Delta$ components in nuclei electron-deuteron scattering at high momentum transfer might be an extremely useful tool.

Electron-deuteron scattering including Δ admixture has been studied already at low momentum transfer[10] with the result of a considerable contribution of the baryonic components. In these calculations the $\Delta\Delta$ components of the deuteron have been obtained in a first order perturbative approach. If these results hold one could expect a large effect of Δ admixtures at high momentum transfer.

In the present paper we determine the deuteron wave function with the inclusion of resonances by a full coupled channel calculation of all partial wave components. A solution of such a coupled channel problem has been achieved already by some people.[11-13] Arenhövel,[11] for example, has solved the coupled channel problem in momentum space. Although we solve the equations in coordinate space our treatment is very similar to that of Arenhövel.

In Sec. II we present our model for the description of the deuteron and discuss different possibilities for the partial waves arising from the sensitivity of the treatment from the choices of baryon-baryon interactions. In Sec. III we calculate the electromagnetic form factors of the deuteron as determined in Sec. II. As far as the meson-exchange currents are concerned we include π, ρ, ω, and $\rho\pi\gamma$ exchange. As the explicit form of these currents are given in Ref. 5 we do

not discuss them again. In Sec. IV, however, we discuss these processes together with the resonance contributions to the deuteron form factors.

II. DEUTERON WAVE FUNCTIONS WITH RESONANCE ADMIXTURES

In the determination of the deuteron wave function we start with the "conventional" nonrelativistic Schrödinger equation including resonance Δ (1236 MeV) degrees of freedom:

$$H\Psi = E\Psi . \tag{1}$$

The total Hamiltonian H consists of a pure nucleon part (H_N), a pure resonance part (H_Δ), and a transition interaction ($H_{N\Delta}$) which can be written as follows:

$$H_N = \frac{\vec{p}^2}{m_N} + v_{NN\to NN} , \tag{2}$$

$$H_\Delta = \frac{\vec{p}^2}{m_\Delta} + v_{\Delta\Delta\to\Delta\Delta} + \delta , \tag{3}$$

$$H_{N\Delta} = v_{NN\leftrightarrow\Delta\Delta} , \tag{4}$$

where the constant δ is given by

$$\delta = 2(m_\Delta - m_N) , \tag{5}$$

and $\vec{p}$ is the relative momentum of two particles. The Schrödinger equation (1) can be written in a matrix form as

$$\vec{\nabla}^2 \begin{pmatrix} \Psi_N \\ \Psi_\Delta \end{pmatrix} = \begin{pmatrix} m_N(v_{NN\to NN} - E) & m_N v_{NN\leftrightarrow\Delta\Delta} \\ m_\Delta v_{NN\leftrightarrow\Delta\Delta} & m_\Delta[v_{\Delta\Delta\to\Delta\Delta} - (E-\delta)] \end{pmatrix} \begin{pmatrix} \Psi_N \\ \Psi_\Delta \end{pmatrix} , \tag{6}$$

where Ψ_N is the nucleonic component

$$\Psi_N = \sum_{\substack{L=0\ S=1,\\ L=2\ S=1}} \frac{1}{r} u_{LS}(r) \,|\, N^2(LS)J=1, T=0\rangle \tag{7}$$

and Ψ_Δ the resonance component

$$\Psi_\Delta = \sum_{LS} \frac{1}{r} u^*_{LS}(r) \,|\, \Delta^2(LS)J=1, T=0\rangle . \tag{8}$$

From selection rules we have four resonance ($\Delta\Delta$) channels, namely, $^3S_1^*$, $^3D_1^*$, $^7D_1^*$, and $^7G_1^*$.

The normalization of the wave function is put to unity as

$$\int_0^\infty dr(|u_{01}|^2 + |u_{21}|^2 + |u^*_{01}|^2 + |u^*_{21}|^2 + |u^*_{23}|^2 + |u^*_{43}|^2) = 1 . \tag{9}$$

Model potentials

As for the nucleon-nucleon (NN) potential [Fig. 1(a)] we chose a modified Reid-soft-core potential by introducing a parameter β in the central part of the triplet channel:

$$V_c = -10.463\, e^{-x}/x + 105.468\, e^{-2x}/x - \beta\, 3187.8\, e^{-4x}/x + 9924.3\, e^{-6x}/x . \tag{10}$$

The tensor interaction will be left unchanged.

In the pure NN case β is equal to one. In the presence of $\Delta\Delta$ components β is adjusted to give the correct binding energy of the deuteron. This choice has been taken earlier by other people.[11,14] The modification of the intermediate-range attraction as in Eq. (10) may be justified by the fact that the $\Delta\Delta$ components give rise to a similar interaction.[17,18]

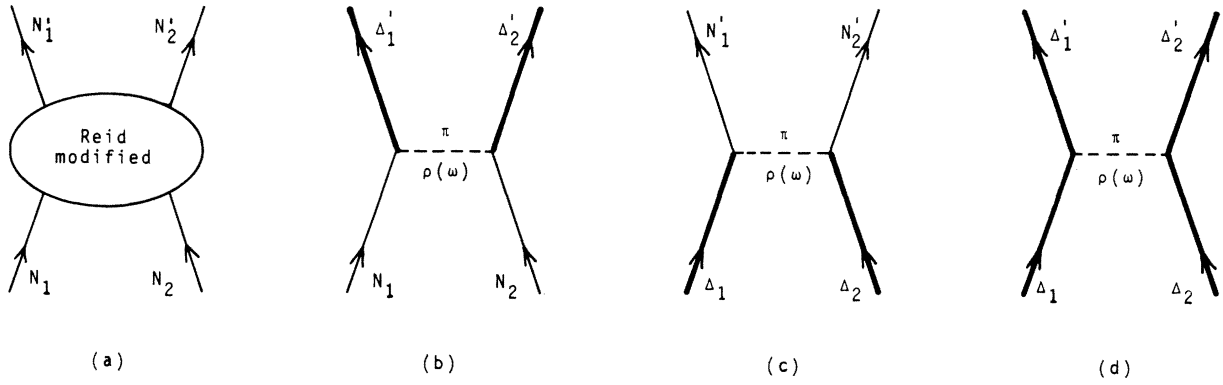

FIG. 1. Illustration of the baryon-baryon potentials taken into account. Diagram (a) corresponds to the modified Reid-soft-core nucleon-nucleon potential [see Eq. (10)]. Diagrams (b) and (c) illustrate the $NN \longleftrightarrow \Delta\Delta$ transition potential, whereas diagram (d) corresponds to the $\Delta\Delta$ interaction.

As for the $\Delta\Delta$ [Fig. 1(d)] and $NN \rightleftharpoons \Delta\Delta$ [Figs. 1(b) and 1(c)] transition potentials we derived one-boson-exchange potentials due to π, ρ, and ω exchange. For the meson-nucleon vertices we used the monopole form factors. The ω-exchange part in the interaction $v_{\Delta\Delta\leftrightarrow\Delta\Delta}$ gave rise to an unphysically high probability in the $^3S_1^*$ and $^3D_1^*$ channels (3–8%). Instead of a further modification of the short-range part of the interaction we simply dropped the ω-exchange part. The potentials used in the numerical calculations have the following forms:

$$v_{NN\leftrightarrow\Delta\Delta} = (\vec{\tau}^{(1)}_{N\Delta}\cdot\vec{\tau}^{(2)}_{N\Delta})\,(\vec{\sigma}^{(1)}_{N\Delta}\cdot\vec{\sigma}^{(2)}_{N\Delta}\,V_C^{N\Delta}+S_{12}^{N\Delta}\,V_T^{N\Delta})\,, \tag{11}$$

$$v_{\Delta\Delta\rightarrow\Delta\Delta} = (\vec{\tau}^{(1)}_{\Delta\Delta}\circ\vec{\tau}^{(2)}_{\Delta\Delta})\,(V_S^{\Delta\Delta}+\vec{\sigma}^{(1)}_{\Delta\Delta}\cdot\vec{\sigma}^{(2)}_{\Delta\Delta}\,V_C^{\Delta\Delta}+S_{12}^{\Delta\Delta}\,V_T^{\Delta\Delta}) \tag{12}$$

with

$$V_C^{B_1B_2} = V_C^{B_1B_2\pi}(m_\pi r)+2V_C^{B_1B_2\rho}(m_\rho r)\,, \tag{13}$$

$$V_T^{B_1B_2} = V_T^{B_1B_2\pi}(m_\pi r)-V_T^{B_1B_2\rho}(m_\rho r)\,, \tag{14}$$

$$B_1B_2 \equiv N\Delta \text{ or } \Delta\Delta\,,$$

and

$$V_C^{B_1B_2\alpha}(m_\alpha r) = \tfrac{1}{3}m_\alpha\frac{f^2_{B_1B_2\alpha}}{4\pi}\left[Y_0(m_\alpha r)-\frac{\Lambda}{m_\pi}Y_0(\Lambda r)\left(1+\frac{\Lambda^2-m_\alpha^2}{2\Lambda^2}\Lambda r\right)\right], \tag{15}$$

$$V_T^{B_1B_2\alpha}(m_\alpha r) = \tfrac{1}{3}m_\alpha\frac{f^2_{B_1B_2\alpha}}{4\pi}\left[Y_2(m_\alpha r)-\left(\frac{\Lambda}{m_\alpha}\right)^3 Y_2(\Lambda r)+\frac{\Lambda}{m_\alpha}\frac{\Lambda^2-m_\alpha^2}{2m_\alpha^2}\Lambda r\,Y_1(\Lambda r)\right], \tag{16}$$

$$V_S^{\Delta\Delta}(m_\rho r) = -\frac{g^2_{\Delta\Delta\rho}}{4\pi}m_\rho\left[Y_0(m_\rho r)-\frac{\Lambda}{m_\rho}Y_0(\Lambda r)\left(1+\frac{\Lambda^2-m_\rho^2}{2\Lambda^2}\Lambda r\right)\right]. \tag{17}$$

Here we defined

$$Y_0(x) = e^{-x}/x,\quad Y_1(x) = (1+1/x)\,e^{-x}/x\,,$$
$$Y_2(x) = (1+3/x+3/x^2)\,e^{-x}/x\,, \tag{18}$$

and α denotes π or ρ. Λ is the parameter associated with the monopole meson-nucleon form factor.

The operators $\vec{\sigma}_{N\Delta}$ and $\vec{\tau}_{N\Delta}$ are the transition spin and isospin operators defined by

$$\langle\tfrac{3}{2}\|\vec{\sigma}_{N\Delta}\|\tfrac{1}{2}\rangle = \langle\tfrac{3}{2}\|\vec{\tau}_{N\Delta}\|\tfrac{1}{2}\rangle = 2\,. \tag{19}$$

The operators $\vec{\sigma}_{\Delta\Delta}$ and $\vec{\tau}_{\Delta\Delta}$ are defined by

$$\langle\tfrac{3}{2}\|\vec{\sigma}_{\Delta\Delta}\|\tfrac{3}{2}\rangle = \langle\tfrac{3}{2}\|\vec{\tau}_{\Delta\Delta}\|\tfrac{3}{2}\rangle = 2\sqrt{15}\,. \tag{20}$$

The tensor operators $S_{12}^{B_1B_2}$ are defined in the usual way as

$$S_{12}^{B_1B_2} = \frac{3}{r^2}(\vec{\sigma}^{(1)}_{B_1B_2}\circ\vec{r})\,(\vec{\sigma}^{(2)}_{B_1B_2}\cdot\vec{r})-\vec{\sigma}^{(1)}_{B_1B_2}\cdot\vec{\sigma}^{(2)}_{B_1B_2}\,. \tag{21}$$

The meson-baryon coupling constants used are summarized in Table I.

Numerical calculation

For solving the six coupled equations [Eq. (6)] we adopted the Numerov algorithm.[15] Details are given in Appendix A. We checked our program by several solvable models for three coupled channels. The solvable models are explicitly given in Appendix B.

TABLE I. Meson-baryon coupling constants used throughout in this work.

$f^2_{\Delta N\pi}/4\pi$	$f^2_{\Delta N\rho}/4\pi$	$f^2_{\Delta\Delta\pi}/4\pi$	$f^2_{\Delta\Delta\rho}/4\pi$	$g^2_{\Delta\Delta\rho}/4\pi$
0.36	9.24	0.0032	0.131	0.89

In Table II we give the probabilities of the deuteron components calculated by different potentials. We take two different choices for the monopole form factor, namely, $\Lambda^2 = 1.1$ GeV^2 and $\Lambda^2 = 1.91$ GeV^2. For each Λ we calculated the wave functions with four different choices of potentials. Cases 1 and 5 show the results calculated with a one-pion exchange in the $NN \rightleftharpoons \Delta\Delta$ transition potential and no interaction in the $\Delta\Delta$ channel. Cases 2 and 6 are calculated by a transition interaction mediated by π and ρ exchange, and again no interaction in the $\Delta\Delta$ channel. Cases 3 and 7 include in the transition potential and in the $\Delta\Delta$ interaction the exchange of one π only. Cases 4 and 8 include π and ρ exchange in the transition potential as well as in the $\Delta\Delta$ interaction. The total probability of $\Delta\Delta$ admixtures strongly depends on the meson-nucleon form factor. For $\Lambda^2 = 1.1$ GeV^2 the total probability is around 0.69–0.76%; for $\Lambda^2 = 1.91$ GeV^2 the total probability is roughly twice as large (1.05–1.53%). In both cases of meson-nucleon form factors the $^7D_1^*$ component is by far the most important component. This is due to the fact that in this channel the tensor force is most effective. The partial wave components are not very sensitive to the choice of the potentials, except for the $^3S_1^*$ channel. The only earlier calculations of admixtures obtained by solutions of coupled equations are the recent ones of Arenhövel.[11] The overall feature

TABLE II. Deuteron $\Delta\Delta$ probabilities for different meson-exchange processes and different meson-nucleon form factors.

No.	$V_{NN-\Delta\Delta}$	$V_{\Delta\Delta-\Delta\Delta}$	Λ^2 (GeV^2)	β	$P_{\Delta\Delta}$ (%) $^3S_1^*$	$^3D_1^*$	$^7D_1^*$	$^7G_1^*$	Total	P_{NN} (%) $^3D_1$
1	π	No	1.1	0.8316	0.025	0.020	0.663	0.056	0.764	6.03
2	π, ρ	No	1.1	0.8470	0.062	0.024	0.568	0.050	0.704	6.09
3	π	π	1.1	0.8432	0.077	0.028	0.531	0.056	0.693	6.12
4	π, ρ	π, ρ	1.1	0.8439	0.126	0.036	0.540	0.054	0.756	6.15
5	π	No	1.91	0.7216	0.038	0.033	1.202	0.088	1.36	5.92
6	π, ρ	No	1.91	0.7843	0.162	0.043	0.782	0.065	1.05	6.09
7	π	π	1.91	0.7450	0.249	0.073	0.871	0.093	1.29	6.11
8	π, ρ	π, ρ	1.91	0.7500	0.379	0.079	0.985	0.084	1.53	6.14

of the probabilities looks similar, but in some cases there are some considerable differences. One example to compare is our case 5 with his case 8. Except for the $^3D_1^*(\Delta\Delta)$ channel the probabilities of the other channels are generally larger than ours (total probability 1.87% compared with our result 1.36%). In contrast to Ref. 11 we do not observe a general decrease of the $(\Delta\Delta)$ probability with the inclusion of the $\Delta\Delta$ interaction.

All the results shown are those without the inclusion of the ω exchange. The reason for this is that including the ω exchange we obtained unphysically high $\Delta\Delta$ probabilities. This is caused by the sensitivity of the $^3S_1^*(\Delta\Delta)$ channel to the short range behavior of the potentials.

Some wave functions are shown in Figs. 2–6. The *NN* wave functions are shown in Fig. 2 for comparison. The figures show clearly the sensi-

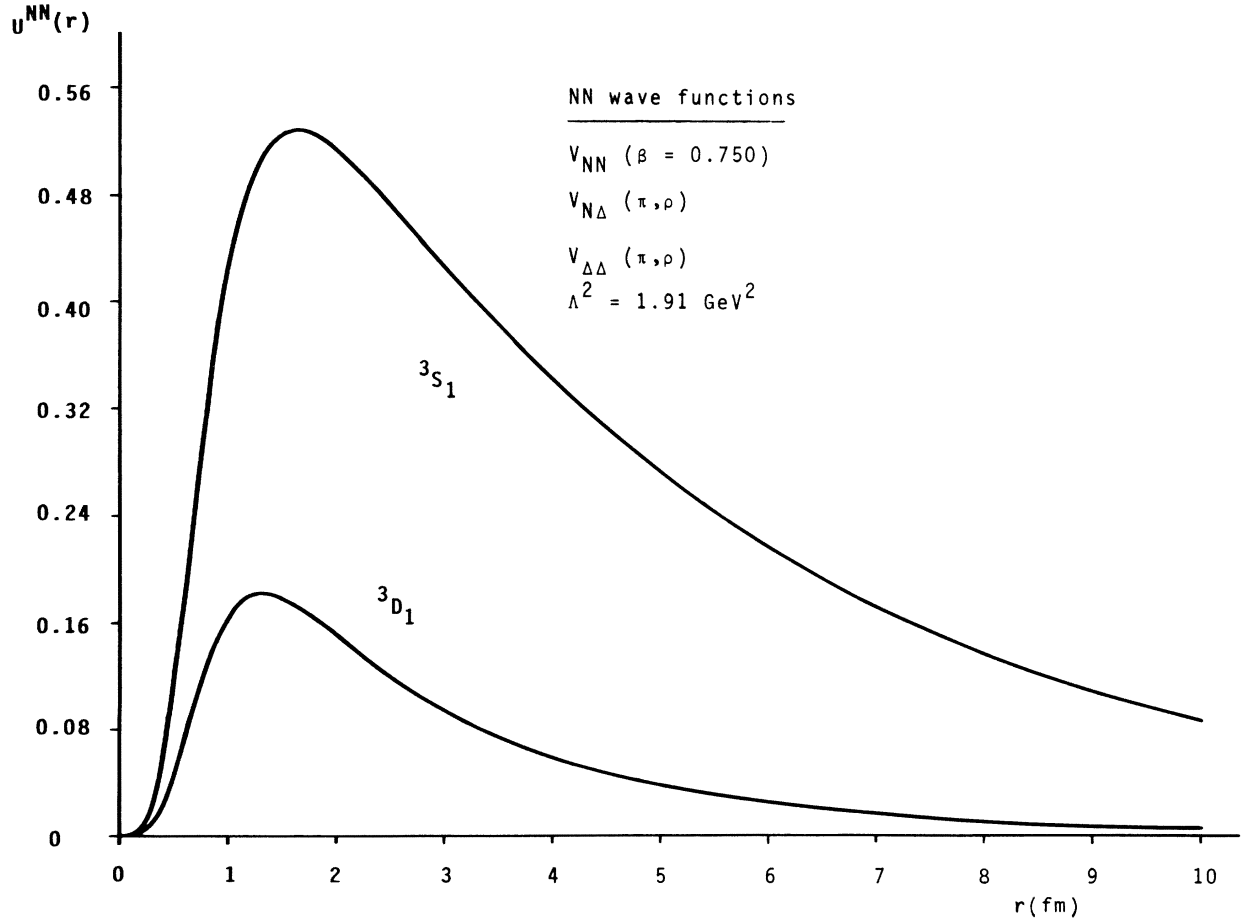

FIG. 2. Nucleonic components of the deuteron wave functions corresponding to case (4) of Table II.

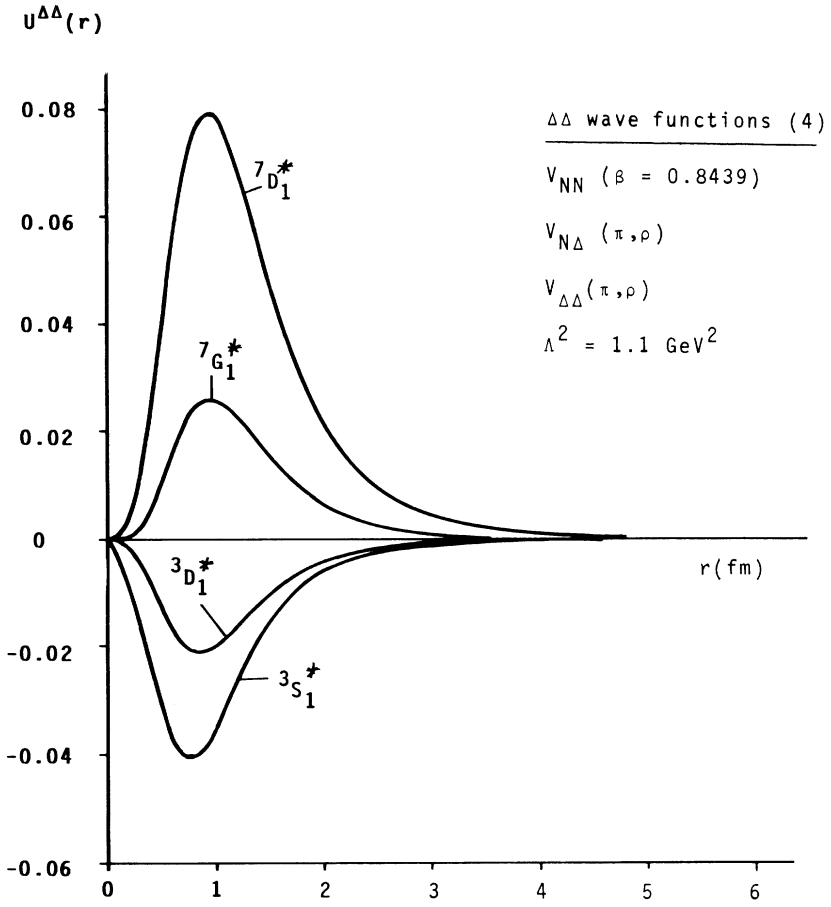

FIG. 3. Resonance partial wave components of the deuteron for case (4) of Table II.

tivity of the $^3S_1^*(\Delta\Delta)$ component on the choice of the potentials.

III. ELECTROMAGNETIC FORM FACTOR OF THE DEUTERON

In the calculation of the deuteron form factor we follow Gari and Hyuga[4,5] in the treatment of meson-exchange currents, i.e., we include the exchange of π, ρ, ω, and $\rho\pi\gamma$. For details of the treatment of the exchange currents we refer to Refs. 4 and 5. The total contributions to be included in this paper are diagrammatically shown in Figs. 7(a)–7(c). There are certainly additional meson-exchange currents associated with the ΔΔ components of the wave function as illustrated in Figs. 8(a)–8(c). These contributions seem to be not important as the leading piece, the pion pair current, is strongly suppressed in the present case.

The form factors are defined by the following cross section of electron-deuteron scattering:

$$\frac{d\sigma}{d\Omega} = \left(\frac{d\sigma}{d\Omega}\right)_{\text{Mott}} \times\left(F_E^{\,2}(q^2) + [1 + 2\tan^2(\tfrac{1}{2}\theta)]\frac{q^2}{m_N^{\,2}}F_M^{\,2}(q^2)\right) \tag{22}$$

with

$$F_E^{\,2}(q^2) = F_C^{\,2}(q^2) + \tfrac{1}{18}q^4F_Q^{\,2}(q^2)\,, \tag{23}$$

where q is the electron momentum transfer and F_C, F_Q, and F_M are the charge, quadrupole, and magnetic form factors. According to our description the form factors consist of three contributions:

$$F_X(q^2) = F_X^N(q^2) + F_X^\Delta(q^2) + F_X^{\text{EXC}}(q^2)\,. \tag{24}$$

The first term corresponds to diagram (a) in Fig. 7, the second and third terms to diagrams (b) and (c), respectively.

The form factors $F_X^N(q^2)$ and $F_X^{\text{EXC}}(q^2)$ are explicitly given in Ref. 5. The only difference

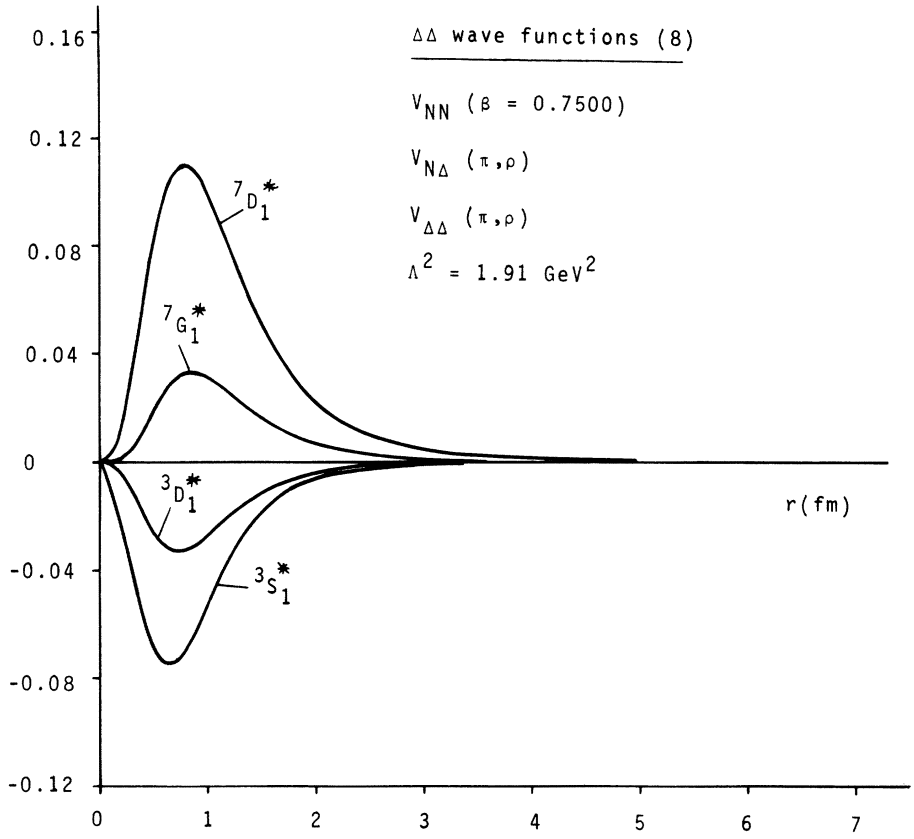

FIG. 4. Resonance partial wave components of the deuteron for case (8) of Table II.

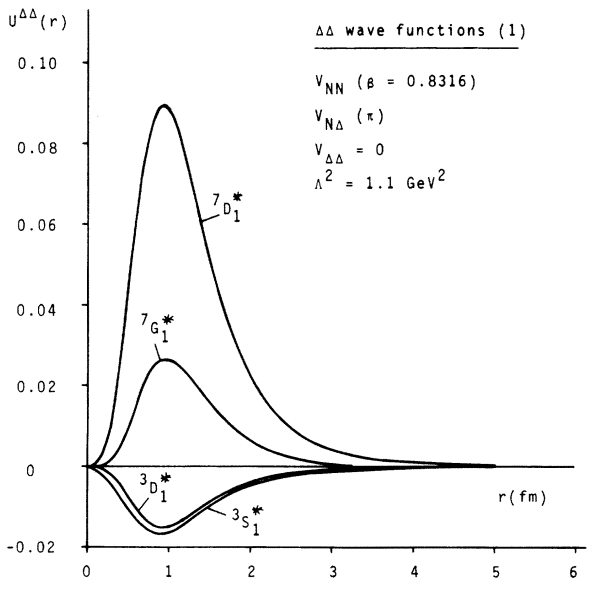

FIG. 5. Resonance partial wave components of the deuteron for case (1) of Table II.

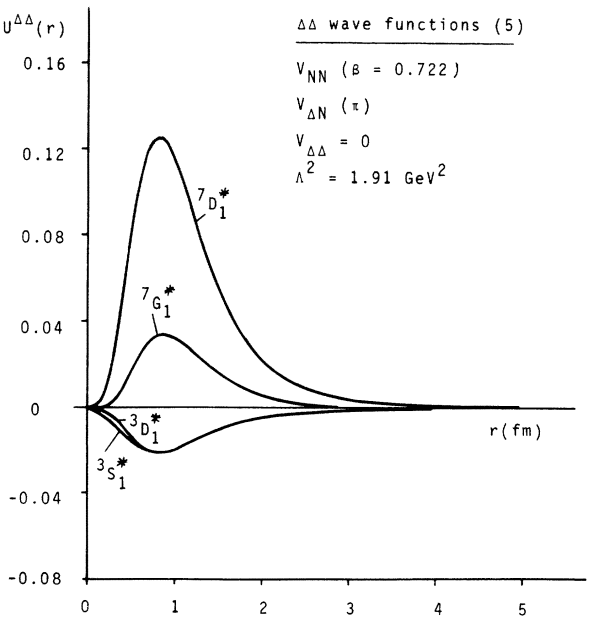

FIG. 6. Resonance partial wave components of the deuteron for case (5) of Table II.

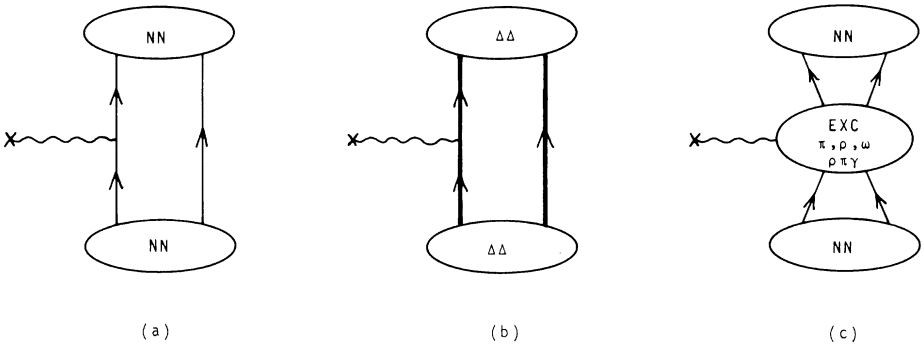

FIG. 7. Electromagnetic interaction processes taken into account in the calculation of the deuteron form factors. Diagrams (a) and (b) illustrate the impulse approximation contributions from the nucleonic and resonance parts of the wave function. Diagram (c) corresponds to the meson-exchange currents included in the present calculations.

arises from the definition of the deuteron wave function [Eqs. (7–9)] as the interpretation of the nucleonic component of the wave function is different.

Introducing the simplifying notation for the wave function Eq. (8):

$$u_1 \equiv u_{01},\quad u_2 = u_{21},\quad u_1^* = u_{01}^*,\quad u_2^* = u_{21}^*,\quad u_3^* = u_{23}^*,\quad u_4^* = u_{43}^*, \tag{25}$$

the $\Delta\Delta$ contribution of the deuteron to the form factors F_C, F_Q, and F_M can be summarized as follows:

$$F_C^{\Delta}(q^2) = G_E^S(q^2) \int_0^{\infty} dr\, j_0(\tfrac{1}{2}qr)\left[(u_1^*)^2 + (u_2^*)^2 + (u_3^*)^2 + (u_4^*)^2\right], \tag{26}$$

$$F_Q^{\Delta}(q^2) = \frac{3}{q^2} G_E^S(q^2) \int_0^{\infty} dr\, j_2(\tfrac{1}{2}qr)\left[2\sqrt{2}\,u_1^* u_2^* - (u_2^*)^2 - \tfrac{2}{7}(u_3^*)^2 + (12\sqrt{3}/7)\,u_3^* u_4^* - \tfrac{5}{7}(u_4^*)^2\right], \tag{27}$$

$$\begin{aligned} F_M^{\Delta}(q^2) = {} & \frac{m_N}{m_{\Delta}} G_E^S(q^2) \int_0^{\infty} dr\left[j_0(\tfrac{1}{2}qr) + j_2(\tfrac{1}{2}qr)\right]\left[\tfrac{3}{4}(u_2^*)^2 - \tfrac{2}{4}(u_3^*)^2 + \tfrac{5}{4}(u_4^*)^2\right] \\ & + G_M^S(q^2) \int_0^{\infty} dr\, j_0(\tfrac{1}{2}qr)\left[(u_1^*)^2 - \tfrac{1}{2}(u_2^*)^2 + 2(u_3^*)^2 - \tfrac{3}{2}(u_4^*)^2\right] \\ & + G_M^S(q^2) \int_0^{\infty} dr\, j_2(\tfrac{1}{2}qr)\left[1/\sqrt{2}\,u_1^* u_2^* + \tfrac{1}{2}(u_2^*)^2 - \tfrac{4}{7}(u_3^*)^2 (3\sqrt{3}/7)\,u_3^* u_4^* + \tfrac{15}{14}(u_4^*)^2\right]. \end{aligned} \tag{28}$$

Here $G_E^S(q^2)$ and $G_M^S(q^2)$ are isoscalar electric and magnetic form factors. They are taken from Iachello, Jackson, and Landé (IJL) with a different normalization: $F_1^S(0) = 1$.

In the derivation of the electromagnetic interaction of the resonance we simply used the static quark model and the scaling assumption.

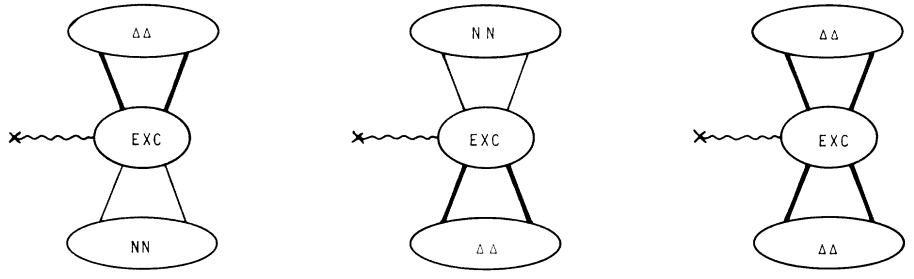

FIG. 8. Illustration of other types of meson-exchange currents also contributing to the deuteron form factors. They are neglected in the present work as their leading terms are suppressed.

IV. NUMERICAL RESULTS

In Figs. 9–11 we show the individual contributions of the exchange currents ($\pi, \rho, \omega, \rho\pi\gamma$) and the $\Delta\Delta$ contribution. We showed here the $\Delta\Delta$ contribution together with the individual exchange currents as the $\Delta\Delta$ contribution may be regarded as a two-pion-exchange process. For momentum transfer $q^2 > 20$ fm^{-2} the resonance contribution is comparable to the small contribution of the ρ and ω exchange. As for the magnetic form factor the resonance contribution turns out to be relatively large.

The exchange current contribution shows essentially the same effect as in our earlier calculations where resonance degrees of freedom are not explicitly taken into account. This is due to the small changes in the nucleonic part of the deuteron wave function caused by the presence of resonance freedoms (Fig. 2).

In Figs. 12–16 we show the total charge $F_C(q^2)$, quadrupole $F_Q(q^2)$, magnetic $F_M(q^2)$ form factors as well as $F_E{}^2(q^2)$ and $B(q^2)$. In all figures we show the total impulse results for the form factors [Imp($NN + \Delta\Delta$)] and the contribution of the nucleonic components only, to the impulse form factors [Imp(NN)]. In addition, we show the total impulse plus exchange current form factors ($NN + \Delta\Delta +$ EXC). In all form factors the influence of the resonance degrees of freedom is practically negligible. The same is true for all possible choices of potentials (Table II).

The magnetic moment $F_M(0)$ is of special interest. The individual contributions of the considered processes are summarized in Table III. We compare two cases of deuteron wave functions, namely, case (4) and case (8) of Table II. For comparison we show the results for the Reid-soft-core wave function without resonance components.

The impulse magnetic moment for a deuteron wave function with $\Delta\Delta$ components is given as follows:

NN component:

$$F_M^N(0) = G_M^S(0) + \left[\tfrac{3}{4} - \tfrac{3}{2} G_M^S(0)\right] P_{^3D_1} - G_M^S(0)\, P_{\text{total}}^{\Delta\Delta}; \tag{29}$$

$\Delta\Delta$ *component:*

$$F_M^{\Delta\Delta}(0) = G_M^S(0)\, P_{^3S_1} + \left[\frac{3}{4}\frac{m_N}{m_\Delta} - \tfrac{1}{2} G_M^S(0)\right] P_{^3D_1}^{\Delta\Delta} + \left[-\frac{1}{2}\frac{m_N}{m_\Delta} + 2G_M^S(0)\right] P_{^7D_1}^{\Delta\Delta} + \left[\frac{5}{4}\frac{m_N}{m_\Delta} - \tfrac{3}{2} G_M^S(0)\right] P_{^7G_1}^{\Delta\Delta}. \tag{30}$$

The ($\Delta\Delta$) impulse contribution Eq. (30) is roughly comparable to the contribution of the exchange

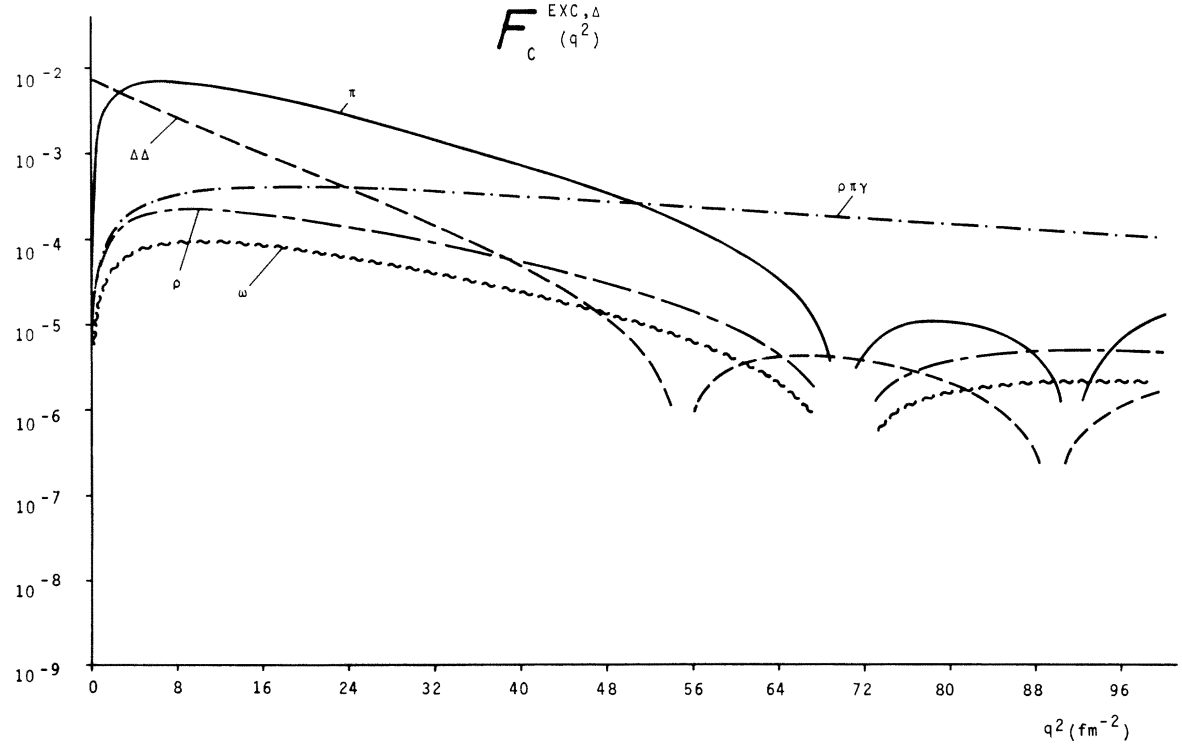

FIG. 9. Comparison of the exchange current (F_C^{EXC}) and resonance (F_C^{Δ}) contributions to the charge form factor.

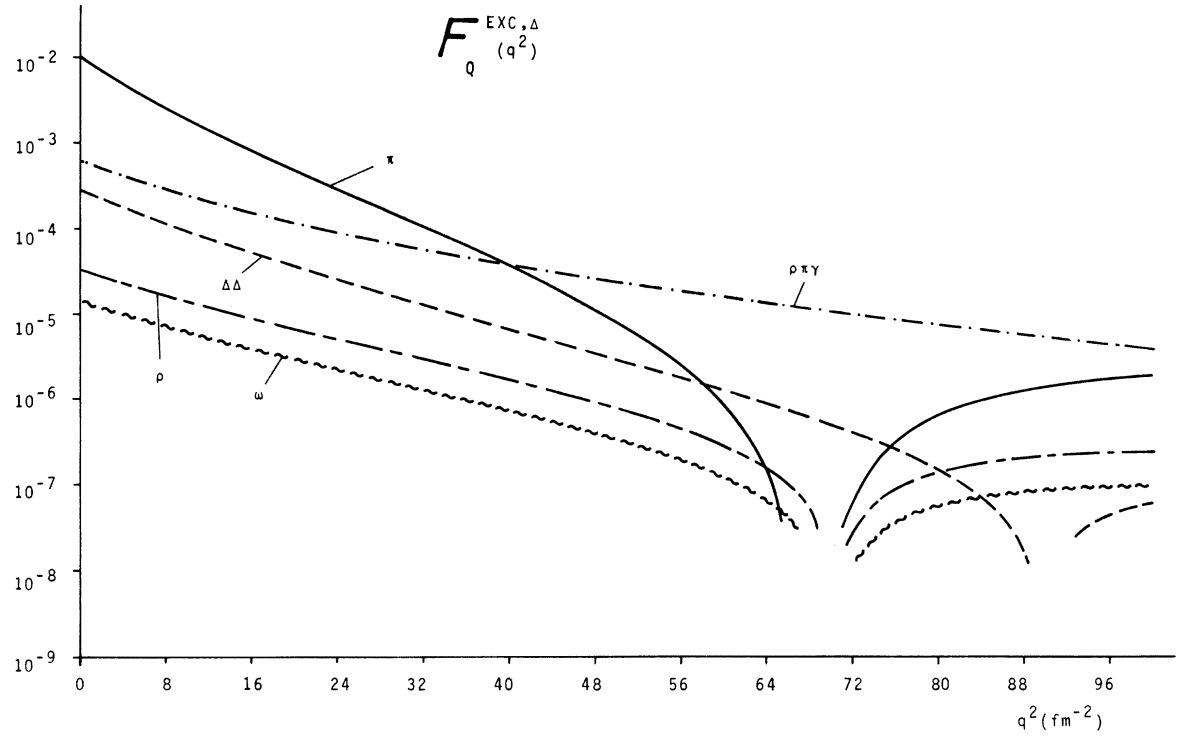

FIG. 10. Comparison of the exchange current (F_Q^{EXC}) and resonance (F_Q^{Δ}) contributions to the quadrupole form factor.

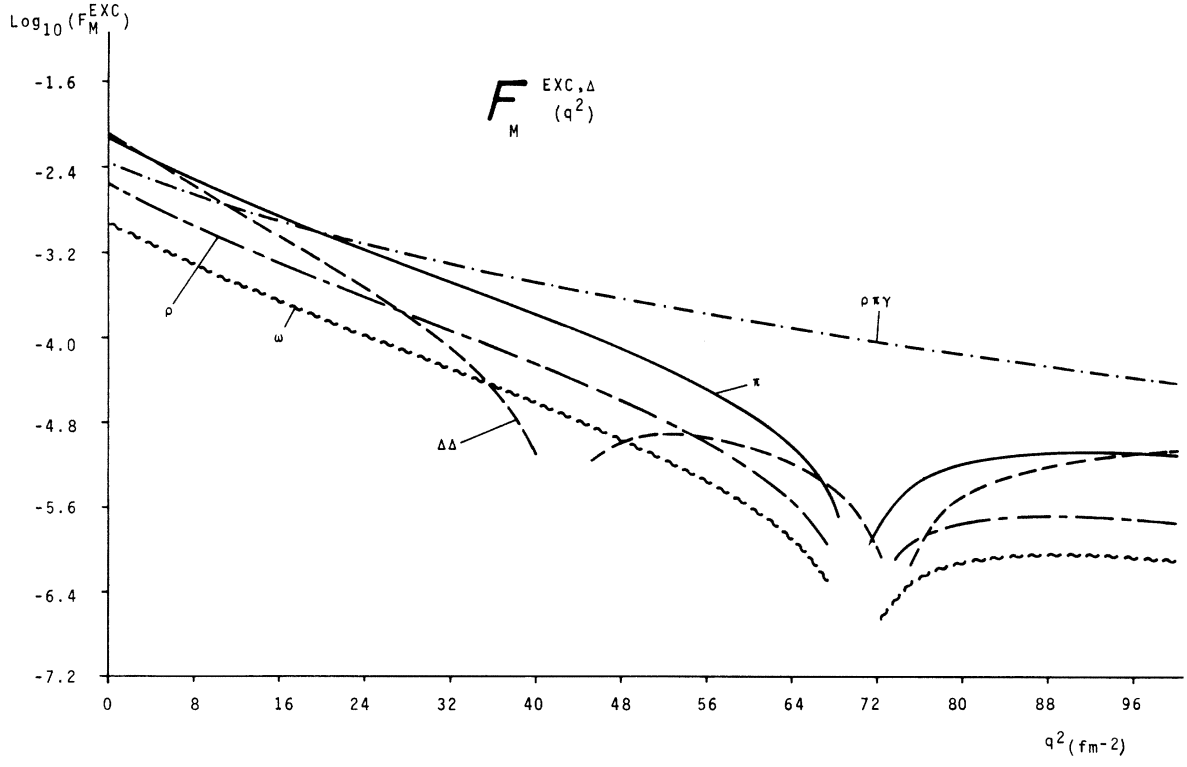

FIG. 11. Comparison of the exchange current (F_M^{EXC}) and resonance (F_M^{Δ}) contributions to the magnetic form factor.

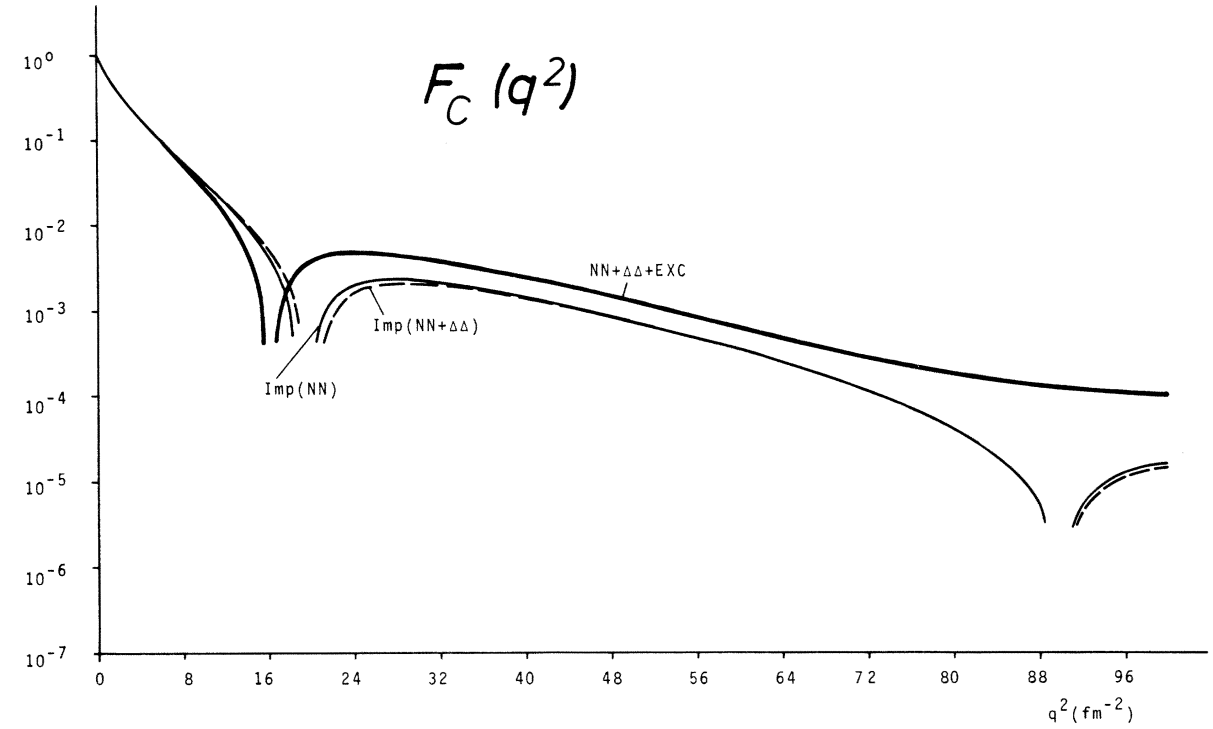

FIG. 12. Total charge form factor $F_C(NN+\Delta\Delta+\text{EXC})$. The total impulse result [Imp$(NN+\Delta\Delta)$] as well as the impulse form factor [$F_C(NN)$] of the nucleonic components, only, are also given.

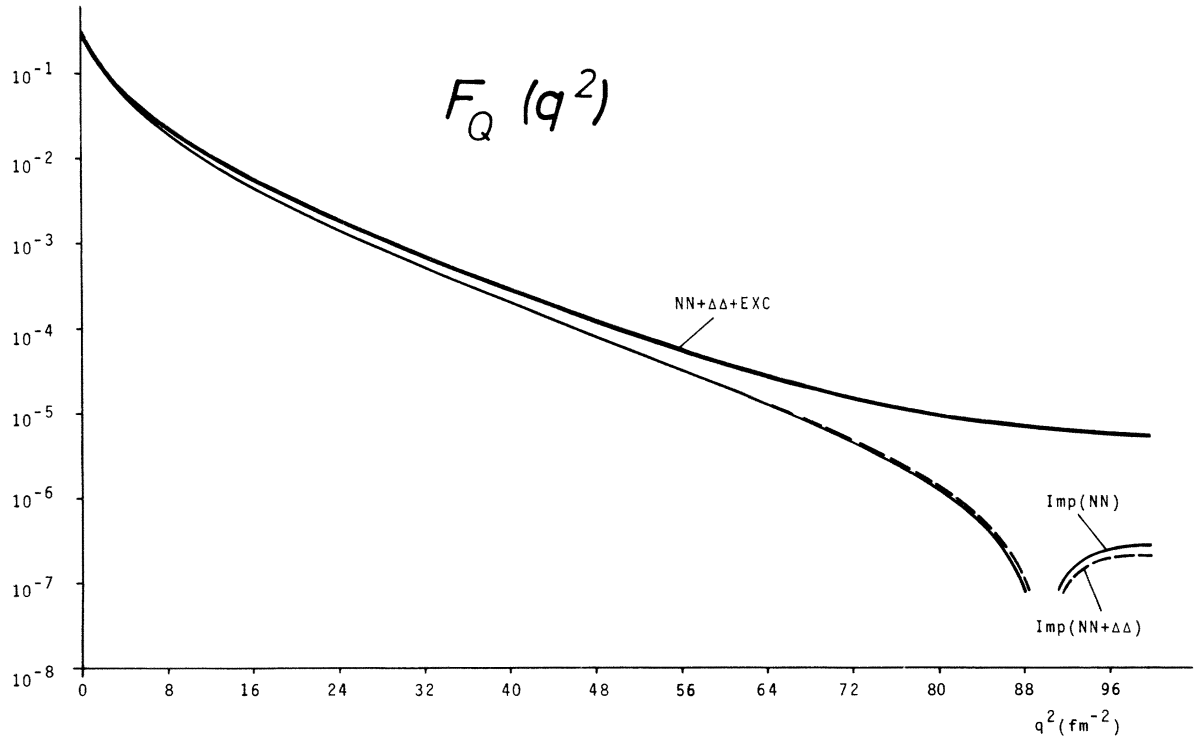

FIG. 13. Total quadrupole form factor $F_Q(NN+\Delta\Delta+\text{EXC})$. The total impulse result [Imp$(NN+\Delta\Delta)$] as well as the impulse form factor $F_Q(NN)$ of the nucleonic components, only, are also given.

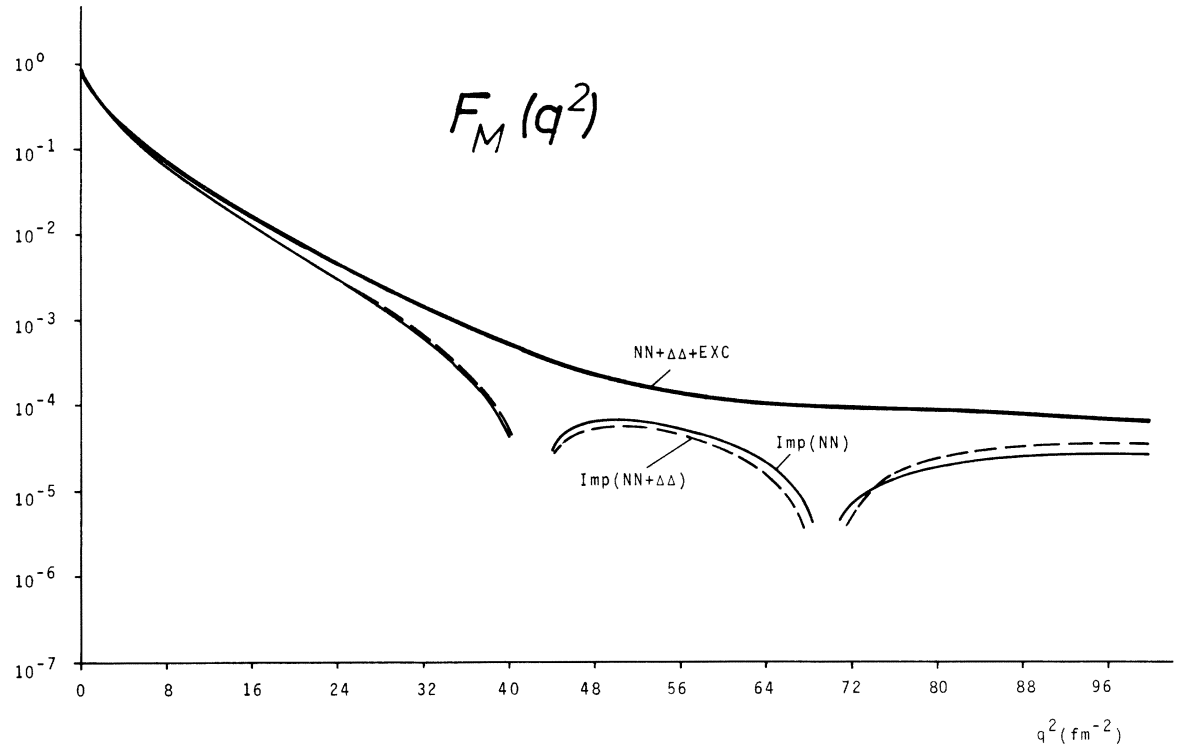

FIG. 14. Total magnetic form factor $F_M(NN+\Delta\Delta+\text{EXC})$. The total impulse result [Imp$(NN+\Delta\Delta)$] as well as the impulse form factor $F_M(NN)$ of the nucleonic components, only, are also given.

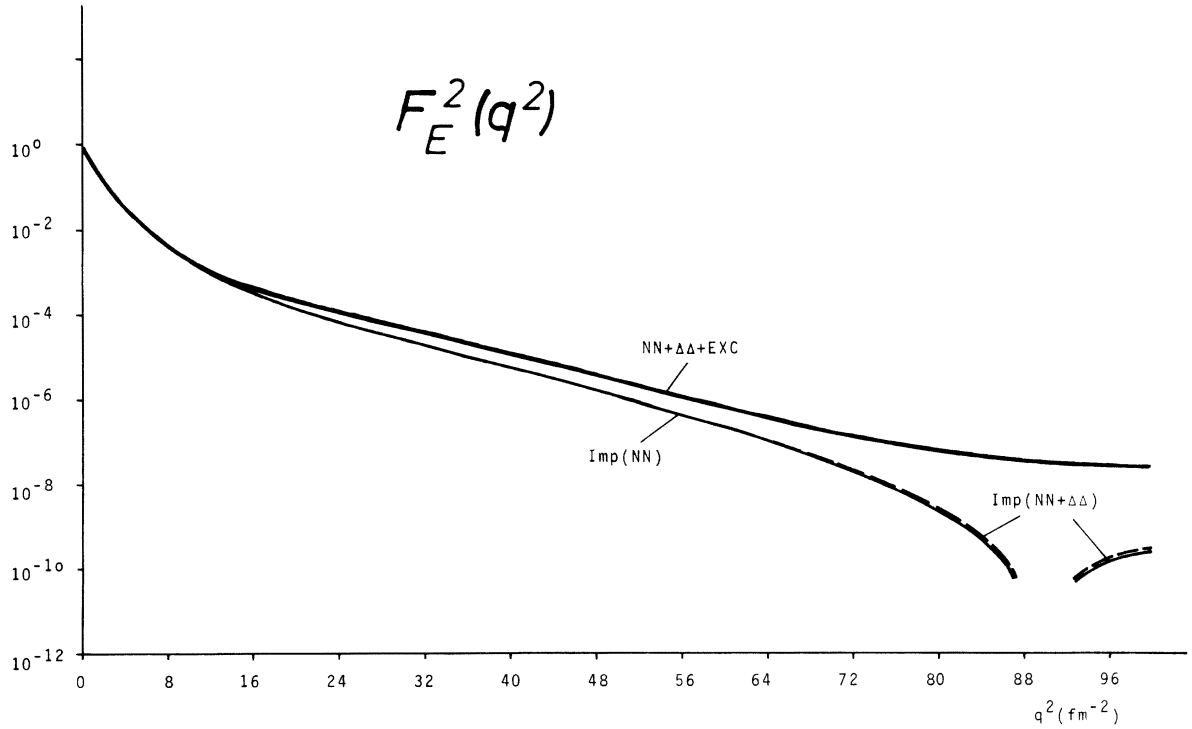

FIG. 15. Total form factor $F_E^2(q^2)$ for $NN+\Delta\Delta+\text{EXC}$. The individual contributions of the total impulse approximation [Imp$(NN+\Delta\Delta)$] and the nucleonic impulse approximation [Imp(NN)] are given.

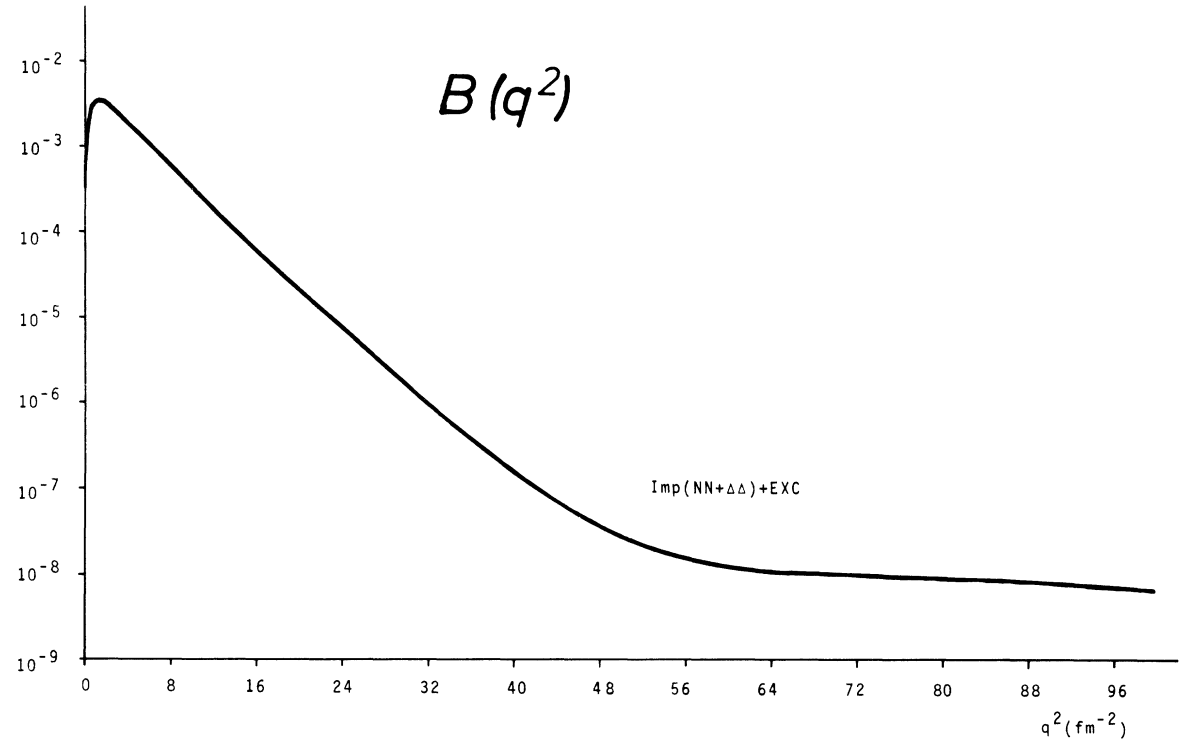

FIG. 16. Deuteron backward scattering form factor $B(q^2) = (q^2/3m_N^2)F_M^2$ with resonance and exchange current contributions.

currents. The main part of the (ΔΔ) impulse contribution arises from the ${}^7D_1^*$ partial wave and roughly explains the difference between case (4) and (8). All the results are very close to the experimental value. The relative insensitivity to the (ΔΔ) contributions arises mainly from the "renormalization effect," namely, the third term of Eq. (29).

V. CONCLUSION

In the present paper we investigated the influence of baryonic degrees of freedom on the electromagnetic form factor. The interest in this problem for us was twofold. Firstly, since the neutron form factors are extracted from the deuteron measurements it is of greatest interest to determine how strongly the baryonic degrees of freedom will invalidate this. A large resonance contribution to the deuteron is likely to spoil the idea of obtaining a reliable neutron form factor from deuteron measurements. Because of the presence of meson-exchange currents such a task is already very difficult. On the other hand, large effects in the deuteron form factor from baryonic resonances could provide an excellent study of such contributions in nuclei. In order to answer some of the questions we solved the full coupled channel problem for the deuteron. As the baryon-baryon potentials are not very well defined at short relative distances (high meson exchange) we discussed the solutions of the equations for many choices of baryon-baryon interactions. The solution of the coupled channel problem has been checked with several solvable models (Appendix B) which makes us confident of the numerical accuracy of our calculation.

TABLE III. The magnetic moment of the deuteron $F_M(0)$ for different descriptions of the deuteron state. The experimental value to be compared with is $F_M^{\text{exp}}(0) = 0.8574\mu_N$.

Deuteron description	Magnetic moment $F_M(0)$ (μ_N) Imp(NN)	Imp(ΔΔ)	EXC	Total
Case (4) Table II ΔΔ(%) = 0.756	0.838	0.008	0.011	0.857
Case (8) Table II ΔΔ(%) = 1.53	0.832	0.017	0.011	0.860
ΔΔ(%) = 0	0.843	···	0.011	0.854

Summarizing the effects of different potentials we note that a large influence on the resonance wave function arises from the choice of the meson-nucleon vertices. Altogether the percentage of resonance (ΔΔ) contributions to the deuteron is in the range of 0.7–1.5% depending on the choice

of meson-nucleon vertices. Except for the $^3S_1^*(\Delta\Delta)$ partial wave the contributions are rather stable concerning the changes in the baryonic interactions.

The influence of the baryonic degrees of freedom on the electromagnetic form factors of the deuteron have been discussed with the variety of deuteron wave functions given in Table II. The calculation of the electromagnetic form factor has been based on the earlier calculations of Refs. 4 and 5, where the meson-exchange currents have been treated in detail.

In the final analysis the effect of the $\Delta\Delta$ resonances in the deuteron turned out to be rather small for all choices of potentials. For the further study of resonance contributions of nuclei by electron-deuteron scattering this result is not very encouraging [we should note in this context that this does not imply a small resonance effect ($T=0$ channel) on the binding energy of nuclei]. However, for the determination of the neutron form factor these findings seem to be of greatest importance.

APPENDIX A: NUMERICAL SOLUTION OF THE SYSTEM OF COUPLED EQUATIONS

The numerical integration of the system of six coupled differential equations has been performed in three steps:
(i) Outward integration u^{out} from the core radius r_c of the potentials to the matching point $\bar{r}=1.4$ fm. The core radius has been chosen as $r_c=0.014$ fm (which is the Reid-soft-core choice) for all baryon-baryon potentials. This integration leads to six linear independent regular solutions

$$\begin{pmatrix}[u(1)]^{\text{out}}\\ [u^*(1)]^{\text{out}}\end{pmatrix},\ \ldots\ \begin{pmatrix}[u(6)]^{\text{out}}\\ [u^*(6)]^{\text{out}}\end{pmatrix}. \tag{A1}$$

$u^{\text{out}}(k)$ and $[u^*(k)]^{\text{out}}$ are two and four component vectors, respectively, as defined in Eq. (25).
(ii) Inward integration from $r=10$ to 5 fm for the nucleonic components only.
(iii) The resonance components are switched on at $r=5$ fm and the full system is integrated up to the matching point $\bar{r}=1.4$ fm. This again gives six independent solutions

$$\begin{pmatrix}[u(1)]^{\text{in}}\\ [u^*(1)]^{\text{in}}\end{pmatrix},\ \ldots\ \begin{pmatrix}[u(6)]^{\text{in}}\\ [u^*(6)]^{\text{in}}\end{pmatrix}. \tag{A2}$$

For the integration procedure we used the Numerov algorithm.[15] At the matching point $\bar{r}=1.4$ fm linear superpositions of the functions u^{in} and u^{out}, respectively (which are continuous at this point), can only be chosen if we are at the exact energy of the system. In general one obtains a discontinuity in the first derivative of one component, say the $^3S_1(NN)$ wave function. This fact can be used to derive an energy correction formula for the eigenvalue problem.[16] In the general case of nonsymmetric potential matrices U_{ij} [Eq. (6)], we split U into a symmetric and antisymmetric part as

$$\begin{aligned} U^S_{ij} &= \tfrac{1}{2}(U_{ij}+U_{ji}),\\ U^A_{ij} &= \tfrac{1}{2}(U_{ij}-U_{ji}) \end{aligned} \tag{A3}$$

and obtain the following correction formula

$$\eta=\frac{2\int_0^\infty dr \sum_{\substack{i=1,2\\ j=1,4}} u_i(\epsilon)\,U^A_{ij}\,u_j^*(\epsilon+\eta)+u_j^*(\epsilon)\,U^A_{ji}\,u_i(\epsilon+\eta)+u_1(\epsilon+\eta)\,\frac{d}{dr}[u_1^{\text{out}}(\epsilon)-u_1^{\text{in}}(\epsilon)]\Big|_{r=\bar{r}}}{\int_0^\infty dr\left\{m_N\left[\sum_{i=1,2}u_i(\epsilon)\,u_i(\epsilon+\eta)\right]+m_\Delta\left[\sum_{i=1,4}u_i^*(\epsilon)\,u_i^*(\epsilon+\eta)\right]\right\}}; \tag{A4}$$

here we have put $\epsilon=Em_N$ and $u(\epsilon)$ is the wave function for the energy ϵ. The derivation of Eq. (14) assumes that $\epsilon'=\epsilon+\eta$ is the correct eigenvalue, so that

$$\frac{d}{dr}[u_1^{\text{out}}(\epsilon+\eta)-u_1^{\text{in}}(\epsilon+\eta)]\Big|_{r=\bar{r}}=0. \tag{A5}$$

APPENDIX B

In order to check the numerical accuracy of our coupled channel calculations we performed solvable model calculations. We assume three channels, namely, an S wave for the nucleon channel $[u(r)]$ and S-wave $[u^*(r)]$ and D wave $[w^*(r)]$ channels for the resonance components. We define first the operators

$$\begin{aligned} T_1&=\frac{d^2}{dr^2}-\alpha^2-m_N V_{11},\\ T_2&=\frac{d^2}{dr^2}-\beta^2-m_\Delta V_{22},\\ T_3&=\frac{d^2}{dr^2}-\frac{6}{r^2}-\beta^2-m_\Delta V_{33}, \end{aligned} \tag{B1}$$

where α and β are given as

$$\alpha=(-m_N E)^{1/2},\quad \beta=[m_\Delta(\delta-E)]^{1/2} \tag{B2}$$

and V_{ij} denote the potentials. Then our coupled channel equation can be written as

$$\begin{aligned} m_N V_{12}u^*+m_N V_{13}w^*&=T_1 u,\\ m_\Delta V_{12}u+m_\Delta V_{23}w^*&=T_2 u^*,\\ m_\Delta V_{13}u+m_\Delta V_{23}u^*&=T_3 w^*. \end{aligned} \tag{B3}$$

We assume the wave functions u, u^*, and w^* to be of the following form:

$$u = e^{-\alpha r} f(r),$$
$$u^* = B_0 e^{-\alpha r} Y(r) f(r), \tag{B4}$$
$$w^* = C_0 e^{-\alpha r} Y(r) F(r) f^4(r),$$

where

$$Y(r) = e^{-m_\pi r}, \quad f(r) = 1 - Y(r)$$

and (B5)

$$F(r) = 1 + \frac{3}{(\alpha + m_\pi) r} + \frac{3}{(\alpha + m_\pi)^2 r^2}.$$

We further assume V_{22} and V_{33} in Eqs. (B1) and (B3) to be zero, then the potentials V_{ij} which solve together with Eq. (B4) the coupled equations (B3) are given as follows:

$$V_{11} = -\frac{m_\pi(2\alpha + m_\pi)}{m_N}\frac{Y(r)}{f(r)} - \frac{Y^2(r)}{m_\Delta f(r)}[B_0^2 V_2(r) + C_0^2 V_3(r)], \tag{B6}$$

$$V_{12} = \frac{Y(r)}{2 m_\Delta B_0 f(r)} \times\{B_0^2[V_2(r) + W_2(r)] + C_0^2[V_3(r) - W_3(r)]\}, \tag{B7}$$

$$V_{13} = \frac{Y(r)}{2 m_\Delta C_0 F(r) f^4(r)} \times\{B_0^2[V_2(r) - W_2(r)] + C_0^2[V_3(r) + W_3(r)]\}, \tag{B8}$$

$$V_{23} = \frac{-1}{2 m_\Delta B_0 C_0 F(r) f^4(r)} \times\{B_0^2[V_2(r) - W_2(r)] + C_0^2[V_3(r) - W_3(r)]\}. \tag{B9}$$

where

$$W_2(r) = c f(r) - d Y(r), \tag{B10}$$
$$W_3(r) = F(r) f^5(r)\{c F(r) f^2(r) - g G(r) f(r) Y(r) + h F(r)[4Y^2(r) - Y(r)]\}, \tag{B11}$$

$$G(r) = 1 + \frac{3}{(\alpha + m_\pi) r} + \frac{6}{(\alpha + m_\pi)^2 r^2} + \frac{6}{(\alpha + m_\pi)^3 r^3} \tag{B12}$$

with the definitions

$$c = (\alpha + m_\pi)^2 - \beta^2, \quad d = m_\pi(2\alpha + 3 m_\pi),$$
$$g = 8 m_\pi(\alpha + m_\pi), \quad h = 4 m_\pi^2. \tag{B13}$$

So far $V_2(r)$ and $V_3(r)$ are arbitrary functions of r. In order to obtain a somewhat realistic case we impose the following conditions on the potentials V_{ij}

$$\text{(i)} \quad V_{ij}(r) \xrightarrow[r\to\infty]{} e^{-m_\pi r}$$
$$\text{(ii)} \quad V_{ij}(r) \xrightarrow[r\to 0]{} O(r^{-1}). \tag{B14}$$

This leads to the following restrictions for V_2 and V_3

$$\text{(i)} \quad V_2(r), V_3(r) \xrightarrow[r\to\infty]{} e^{-m_\pi r},$$
$$\text{(ii)} \quad V_2(r) - W_2(r) \xrightarrow[r\to 0]{} O(r), \tag{B15}$$
$$V_3(r) \xrightarrow[r\to 0]{} O(r).$$

In the actual calculations we took two simple choices which fulfill the conditions Eqs. (B14) and (B15), namely,

case 1:

$$V_2(r) = W_2(r) \quad \text{and} \quad V_3(r) = W_3(r); \tag{B16}$$

case 2:

$$V_2(r) = W_2(r) \quad \text{and} \quad V_3(r) \equiv 0. \tag{B17}$$

The only freedom remaining is then associated with the constants $B_0 C_0$ in Eq. (B4) and the energy of the system E in Eq. (B2).

Our numerical calculations have been checked for both cases Eqs. (B16) and (B17) with various choices for B_0 and C_0 and binding energy E of the system. The accuracy for the binding energy in the numerical calculation actually reached was better than 0.1%.

---

*Work supported by Minister für Wissenschaft und Forschung des Landes Nordrhein-Westfalen, Germany

†Part of this work is part of a thesis.

[1]R. G. Arnold *et al.*, Phys. Rev. Lett. 35, 776 (1975).

[2]M. Chemtob, E. J. Moniz, and M. Rho, Phys. Rev. C 10, 344 (1974).

[3]A. Jackson, A. Landé, and D. O. Riska, Phys. Lett. 55B, 23 (1975).

[4]M. Gari and H. Hyuga, Phys. Rev. Lett. 36, 345 (1976); in *Proceedings of the Seventh International Conference on Few Body Problems in Nuclear and Particle Physics, Delhi, 1975*, edited by A. Mitra (North-Holland, Amsterdam, 1976).

[5]M. Gari and H. Hyuga, Nucl. Phys. A264, 409 (1976).

[6]A. Hamerla, Diplomarbeit, Bochum, 1976 (unpublished).
[7]J. L. Friar, Ann. Phys. (N.Y.) 81, 332 (1973).
[8]F. Coester and A. Ostebee, Phys. Rev. C 11, 1836 (1975).
[9]A. M. Green and P. Haapakoski, Nucl. Phys. A221, 429 (1974); A. Kallio, P. Toropainen, A. M. Green, and T. Kouki, Nucl. Phys. A231, 77 (1974).
[10]H. Arenhövel and H. G. Miller, Z. Phys. A266, 13 (1974).
[11]H. Arenhövel, Z. Phys. A275, 189 (1975).
[12]E. Rost, Nucl. Phys. A249, 510 (1975).
[13]R. A. Smith and V. R. Pandharipande, Nucl. Phys. A256, 327 (1976).
[14]B. Day and F. Coester, Phys. Rev. (to be published).
[15]M. A. Melkanoff, T. Sawada, and J. Raynal, *Methods in Computational Physics* (Academic, New York, 1966), Vol. 6, p. 15.
[16]L. Lovitch and S. Rosati, Phys. Rev. B140, 877 (1965).
[17]H. Sugawara and F. von Hippel, Phys. Rev. 172, 1765 (1968); 185, 2046 (1969).
[18]D. O. Riska and G. E. Brown, Nucl. Phys. A153, 8 (1970).